

MACROSCOPIC ANALYSIS OF THE VISCOUS-DIFFUSIVE TRAFFIC FLOW MODEL

GABRIEL OBED FOSU, ALBERT ADU-SACKEY, AND JOSEPH ACKORA-PRAH

ABSTRACT. Second-order macroscopic traffic models are characterized by a continuity equation and an acceleration equation. Convection, anticipation, relaxation, diffusion, and viscosity are the predominant features of the different classes of the acceleration equation. As a unique approach, this paper presents a new macro-model that accounts for all these dynamic speed quantities. This is done to determine the collective role of these traffic quantities in macroscopic modeling. The proposed model is solved numerically to explain some phenomena of a multilane traffic flow. It also includes a linear stability analysis. Furthermore, the evolution of speed and density wave profiles are presented under the perturbation of some parameters.

1. INTRODUCTION

The main classifications of macroscopic traffic models are the first-order and second-order models [13, 21, 20, 36]. Second-order equations were introduced to overcome the shortcoming of the first-order equation [6, 30]. The first-order category is also known as the continuity or LWR equation. The second-order branch encompasses the first-order equation together with a dynamic velocity equation. Oftentimes the dynamic velocity equation is also called the acceleration or momentum equation. Payne [31] set forth the precedence with his classical dynamic velocity equation with little revision by Whitham [37] some few years afterwards to form the Payne-Whitham (PW) model. The constitutive terms of the acceleration equation are convection, anticipation, relaxation, diffusion, and viscosity. A review of these dynamic terms as either accounted or unaccounted for within a given model formulation is presented in Table 1.

From the reviewed models in Table 1, it was observed that convection, anticipation, and relaxation are always present, but that of diffusion and viscosity are barely modeled. As a novel formulation, all these terms are brought together to form a new momentum equation.

The proposed momentum equation is coupled with the continuity equation to form a system of partial differential equation. Note that each of these terms under consideration describes some realistic traffic phenomena, and hence the need to examine their contributive role in vehicular traffic analysis. The definition and mathematical representation of these terms are detailed in the ensuing paragraphs.

In a traffic sense, the convection or transport term explains the movement of vehicles along with their density/velocity profiles. (A density profile in the case of the continuity equation, and a velocity profile for that of the acceleration equation). These are respectively defined as

$$q'(x, t) \frac{\partial k(x, t)}{\partial x} \quad \text{and} \quad v(x, t) \frac{\partial v(x, t)}{\partial x} \quad (1.1)$$

Received by the editors 24 January 2022; accepted 5 July 2022; published online 9 July 2022.

2010 *Mathematics Subject Classification.* 35Q35, 65M06, 35L40.

Key words and phrases. Second-order model, viscosity, multilane flow, diffusion, speed-density profiles.

TABLE 1. Constituents of the Acceleration Equation

Author(s)	Convection vv_x	Anticipation $(\cdot)k_x$ or $(\cdot)v_x$	Relaxation $(\cdot)(V_e - v)$	Diffusion $(\cdot)v_{xx}$	Viscosity $(\cdot)v_y$
[31]	✓	✓	✓	×	×
[23]	✓		✓	×	×
[25]	✓	✓	✓	✓	×
[28]	✓	✓	✓	×	×
[16]	✓		✓	×	✓
[26]	✓		✓	×	×
[29]	✓	✓	✓	✓	×
[34]	✓		✓	×	×
[38]	✓		✓	✓	×
[39]	✓	✓	✓	×	×
[40]	✓		✓	×	×
[14]	✓	✓	✓	×	✓

$k(x, t)$, $v(x, t)$ and $q(x, t)$ denotes traffic density, speed, and flow rate in that order. The term $v(x, t) \cdot \partial v(x, t) / \partial x$ is to ensure that vehicles do not adjust their speeds in a haste manner. Rather, they are to gradually change their speed to that of the downstream traffic and describes the coordination between the speeds upstream and downstream.

The anticipation term describes the dispersion effect of the speed of heterogeneous traffic. That is, how identical driver-vehicle react to flow conditions in a close neighborhood, more specifically frontal effects. Drivers usually slow down when approaching heavy traffic downstream. The term is a diverging point for most Navier-Stokes-like traffic models. In most Payne-like models, anticipation is modeled by

$$\frac{1}{2\tau k} \frac{dV_e(k)}{dk} \frac{\partial k}{\partial x} \quad \text{or} \quad -\frac{1}{k} \frac{dP(k)}{dk} \frac{\partial k}{\partial x} \quad (1.2)$$

where $P(k) = -V_e(k)/2\tau$ is the pressure term which describes how drivers perceive ahead and adjust to the density downstream. The anticipation term is the core component contributing to the backward traveling wave of Payne-like models. Because of this critique by [9], Aw and Rascle postulated a new pressure term of the form $P(k) = k^\gamma$ with $\gamma > 0$ [3, 32]. However, the AR model was found to be ill-posed for a virtual road [27]. Besides, [23] in their bid to correct the deficiency of negative wave speed replaced the density gradient term with a velocity gradient component, hence defined anticipation as

$$c(k) \frac{\partial v(x, t)}{\partial x} \quad (1.3)$$

The authors specifically used constant $c > 0$ in place of the functional $c(k)$ to denotes the propagation speed of some perturbations.

Another important characterization of traffic is through the relaxation term. This is sometimes called the speed adaptation term. It details how vehicles adapt their speed to the steady-state speed. Given the average speed $v(x, t)$ and $V_e(k)$ the steady-speed as a function of density, then the relaxation term can be defined as

$$\frac{V_e(k(x, t)) - v(x, t)}{\tau} \quad (1.4)$$

This explains how vehicles at average speed could adjust to the situational density-dependent speed. The quantity $\tau > 0$ is the relaxation time for the entire process of adapting to the localized speed. It

is a constant that does not depend on either speed or density. Under normal condition, it is estimated to be between 20 to 30 seconds for highway traffic and something less for urban flow [36].

On certain occasions, the diffusive term

$$D \frac{\partial^2 v(x, t)}{\partial x^2} \quad (1.5)$$

is introduced as part of the macroscopic equations. It was earlier fused into the acceleration equation [25, 29], and later as part of the LWR model [35]. The same expression (Equation 1.5) is used in both the LWR and acceleration equations but may differ in the relevant application. The entire term (1.5) explains how vehicles adjust their velocities to surrounding traffic conditions. It was introduced to smooth shocks and abrupt transitions of traffic between different regimes. That is, smoothing the density profiles in the event of a diffusive first-order model, and smoothing the velocity profile for a diffusive acceleration equation. The diffusive term enhances the numerical properties of the model and also eradicate shockwaves if there is the existence of numerical instabilities.

The last term to discuss is the lateral viscosity term. In the immediate recent past, [16] introduced lateral viscosity to explain traffic resistance on a multilane highway. The term was deduced from the no-slip condition of fluids and is given as

$$s_d \frac{\mu_2}{k(x, t)} \frac{\partial v(x, t)}{\partial y} \quad (1.6)$$

where μ_2 is the lateral viscous rate, s_d is to model the sensitivity of safe vertical distance between vehicles moving on neighboring lanes in the same direction. The velocity gradient $\partial v(x, t)/\partial y$ account for the speed variations with respect to changes in usage of road lanes.

All these terms together with the local derivative $\partial v(x, t)/\partial t$ yields a generalized equation of the form

$$\frac{\partial v(x, t)}{\partial t} + v(x, t) \frac{\partial v(x, t)}{\partial x} = f \left(c(k) \frac{\partial v(x, t)}{\partial x}, c_o^2(k) \frac{\partial k(x, t)}{\partial x}, \frac{V_e(k) - v(x, t)}{\tau}, D \frac{\partial^2 v(x, t)}{\partial x^2}, \phi \frac{\partial v(x, t)}{\partial y} \right) \quad (1.7)$$

f is an arbitrary function, $c_o^2(k) = -\frac{1}{2\tau k(x, t)} \frac{dV_e(k)}{dk}$ and $\phi = s_d \frac{\mu_2}{k(x, t)}$.

Equation (1.7) is decoupled as

$$\frac{\partial v(x, t)}{\partial t} + v(x, t) \frac{\partial v(x, t)}{\partial x} = \frac{V_e(k) - v(x, t)}{\tau} - c_o^2(k) \frac{\partial k(x, t)}{\partial x} + D \frac{\partial^2 v(x, t)}{\partial x^2} - \phi \frac{\partial v(x, t)}{\partial y} \quad (1.8)$$

and

$$\frac{\partial v(x, t)}{\partial t} + v(x, t) \frac{\partial v(x, t)}{\partial x} = c \frac{\partial v(x, t)}{\partial x} + \frac{V_e(k) - v(x, t)}{\tau} + D \frac{\partial^2 v(x, t)}{\partial x^2} - \phi \frac{\partial v(x, t)}{\partial y} \quad (1.9)$$

Equation (1.8) has a density-gradient anticipation term, while (1.9) has a velocity-gradient anticipation term. Equation (1.8) together with the continuity equation is the isotropic viscous-diffusive model. It connotes an extension of all Payne-like models. Equation (1.9) is the anisotropic correspondent.

As stated in Table 1, earlier formulations are devoid of either the diffusion or viscous term. As such, most recent model presentations and analyses also fellow suite [2, 4, 7, 17, 27, 41] with few considering the effect of stochasticity [4, 42]. Concerning traffic stability, the steady-state condition of a viscous second-order macroscopic traffic flow model was performed by [1]. These authors obtained the equilibrium points, the stability criterion, and the phase plane solution of the two velocity difference model (TVDM) [18], which is considered as a simple extension the classical anisotropic macro model. Similarly, [5] conducted a similar analysis to determine the global stability and the bifurcation of a

second-order continuum model. The authors observed the presence of subcritical Hopf bifurcation for their derived macroscopic model. On the other hand, [8] established that the impact of viscosity under a stable traffic condition is approximately zero. These authors used a series of proofs to confirm this near-zero assertion.

This paper also presents a graphical simulation with a stability analysis to determine the effect of both viscosity and diffusion for a multilane traffic flow. The next section begins with a derivation of the instability criterion of a proposed anisotropic model. Specifically, a linearization analysis to determine either stable or unstable traffic flow is presented. It is followed by a numerical simulation; investigating the potency of the model to reproduce some relevant flow phenomena. These simulations are presented within the domain of a multilane infrastructure. The final part of this paper is reserved as the concluding section. However, the analysis concerning the proposed density-gradient model could be considered as future research work.

2. DERIVATION OF INSTABILITY CRITERION

The stability criterion of the proposed model is determined using the linearization technique. Assuming a homogeneous solution $k(x, y, t) = k_e$ and $v(x, y, t) = V_e(k)$. Any deviation from these stationary solutions are given as

$$\delta k = k(x, y, t) - k_e, \quad \text{and} \quad \delta v = v(x, y, t) - V_e(k) \quad (2.1)$$

Consequently, the viscous-diffusive anisotropic macroscopic traffic flow model is linearized as

$$\begin{aligned} \frac{\partial(\delta k)}{\partial t} + V_e \frac{\partial(\delta k)}{\partial x} + k_e \frac{\partial(\delta v)}{\partial x} &= 0 \\ \frac{\partial(\delta v)}{\partial t} + V_e \frac{\partial(\delta v)}{\partial x} - c \frac{\partial(\delta v)}{\partial x} &= \frac{1}{\tau} \left(\frac{dV_e}{dk} \cdot \delta k - \delta v \right) + D \frac{\partial^2(\delta v)}{\partial x^2} - \phi \frac{\partial(\delta v)}{\partial y} \end{aligned} \quad (2.2)$$

By carefully examining vehicle trajectories, it is realized that traffic behaves wave-like. Due to this proposition, the propagation of disturbance of flow can be inferred from the theory of waves. Therefore, the underlying simple wave functions (2.3) is adopted to probe whether a disturbance will escalate or decay over time.

$$\delta k = \hat{k} \exp[is_1 x + is_2 y + (\lambda - i\omega)t] \quad \text{and} \quad \delta v = \hat{v} \exp[is_1 x + is_2 y + (\lambda - i\omega)t] \quad (2.3)$$

$s_{1,2}$ are the spatial wave-numbers. These delimitate the wavelength along the longitudinal and lateral axis respectively, ω is the wave frequency, λ is the wave dumping, \hat{k} and \hat{v} are the amplitudes at some time t .

Further, equation (2.3) and its derivatives are substituted into (2.2). Note that higher order terms are not considered in subsequent computations. The arrived simplification is

$$\begin{aligned} \hat{k}(\lambda - i\omega)\tilde{\mathbb{M}} + iV_e s_i \hat{k} \tilde{\mathbb{M}} + ik_e s_1 \hat{v} \tilde{\mathbb{M}} &= 0 \\ \hat{v}(\lambda - i\omega)\tilde{\mathbb{M}} + (V_e - c)is_1 \hat{v} \tilde{\mathbb{M}} - \frac{\tilde{\mathbb{M}}}{\tau} \left(\frac{dV_e}{dk} \hat{k} - \hat{v} \right) + Ds_1^2 \hat{v} \tilde{\mathbb{M}} + is_2 \hat{v} \tilde{\mathbb{M}} &= 0 \end{aligned} \quad (2.4)$$

where $\tilde{\mathbb{M}} := \exp[is_1 x + is_2 y + (\lambda - i\omega)t] \neq 0$. Equation (2.4) is then represented in its vector form as

$$\begin{bmatrix} \tilde{\lambda} & ik_e s_1 \\ -\frac{1}{\tau} \frac{dV_e}{dk} & \tilde{\lambda} + \frac{1}{\tau} - ics_1 + i\phi s_2 + Ds_1^2 \end{bmatrix} \begin{bmatrix} \hat{k} \\ \hat{v} \end{bmatrix} = \begin{bmatrix} 0 \\ 0 \end{bmatrix} \quad (2.5)$$

This (2.5) is of the typical form $A\hat{x} = 0$. The unknown vector \hat{x} to be determined are the amplitudes $[\hat{k} \ \hat{v}]'$. $\tilde{\lambda} = \lambda - i\omega$ and $\tilde{\omega} = \omega - V_e s_1$ are abbreviations used to alleviate the computational process.

The solution to equation (2.5) is non-trivial if the determinant of the matrix A is zero. The determinant of A produces the quadratic equation:

$$\tilde{\lambda} + \tilde{\lambda} \left(\frac{1}{\check{\tau}} - i\check{\eta} \right) + \frac{i}{\tau} k_e \frac{dV_e}{dk} s_1 = 0 \quad (2.6)$$

where $1/\check{\tau} = 1/\tau + Ds_1^2 > 0$ and $\check{\eta} = cs_1 - \phi s_2 > 0$. The solution to the characteristic polynomial (2.6) is:

$$\tilde{\lambda}_{\pm}(s) = \frac{1}{2} \left(\check{\eta} - \frac{1}{\check{\tau}} \right) \pm \sqrt{\frac{1}{4} \left(\frac{1}{\check{\tau}^2} - \check{\eta}^2 \right) + \left(-\frac{1}{\tau} \frac{dV_e}{dk} k_e s_1 - \frac{\check{\eta}}{2\check{\tau}} \right)} \quad (2.7)$$

As it can be seen, the square root term would yield a complex output, therefore the underlying equation (2.8) is used to simplify this root term. The variable \mathbb{R} is used to denote the real part, while the imaginary part is denoted by \mathbb{I} . From [19]

$$\sqrt{\mathbb{R} \pm i\mathbb{I}} = \sqrt{\frac{1}{2} \left(\sqrt{\mathbb{R}^2 + \mathbb{I}^2} + \mathbb{R} \right)} \pm i \sqrt{\frac{1}{2} \left(\sqrt{\mathbb{R}^2 + \mathbb{I}^2} - \mathbb{R} \right)} \quad (2.8)$$

The discriminant for stability dwells on the real part (Re) of the eigenvalues. Deductively, the real part of the eigenvalues are

$$Re \left(\tilde{\lambda}_{\pm}(s) \right) = -\frac{1}{2\check{\tau}} \pm \sqrt{\frac{1}{2} \left(\sqrt{\mathbb{R}^2 + \mathbb{I}^2} + \mathbb{R} \right)} \quad (2.9)$$

A choice is made between $Re(\tilde{\lambda}_-(s))$ and $Re(\tilde{\lambda}_+(s))$ depending on which is more non-negative. Observably, $Re(\tilde{\lambda}_-(s)) < Re(\tilde{\lambda}_+(s))$, which implies that any condition satisfying $Re(\tilde{\lambda}_+(s))$ will automatically satisfy $Re(\tilde{\lambda}_-(s))$. Hence, the relevant eigenvalue to determine transitions from stationary traffic to unstable flow is $Re(\tilde{\lambda}_+(s))$. That is

$$-\frac{1}{2\check{\tau}} + \sqrt{\frac{1}{2} \left(\sqrt{\mathbb{R}^2 + \mathbb{I}^2} + \mathbb{R} \right)} \geq 0$$

Simplified as

$$\mathbb{I}^2 \geq \frac{1}{4\check{\tau}^4} - \frac{\mathbb{R}}{\check{\tau}^2} \quad (2.10)$$

The result of substituting the values of $\mathbb{R} = \frac{1}{4} \left(\frac{1}{\check{\tau}^2} - \check{\eta}^2 \right)$ and $\pm|\mathbb{I}| = \frac{1}{\tau} \left| \frac{dV_e}{dk} \right| k_e s_1 - \frac{\check{\eta}}{2\check{\tau}}$ into (2.10) is

$$\left(\frac{1}{\tau} \left| \frac{dV_e}{dk} \right| k_e s_1 - \frac{\check{\eta}}{2\check{\tau}} \right)^2 \geq \frac{1}{4\check{\tau}^4} - \frac{1}{4} \frac{1}{\check{\tau}^2} \left(\frac{1}{\check{\tau}^2} - \check{\eta}^2 \right) \quad (2.11)$$

simplified as

$$\frac{1}{\tau} \left| \frac{dV_e}{dk} \right| k_e s_1 \cdot \left(\frac{1}{\tau} \left| \frac{dV_e}{dk} \right| k_e s_1 - \frac{\check{\eta}}{\check{\tau}} \right) \geq 0$$

Finally, the instability condition is obtained as

$$\frac{1}{\tau} \left| \frac{dV_e}{dk} \right| k_e s_1 \geq \frac{\check{\eta}}{\check{\tau}} = (cs_1 - \phi s_2) \left(\frac{1}{\tau} + Ds_1^2 \right) \quad (2.12)$$

The instability condition is gratified if the change in velocity as a result of change in density is quite larger. This scenario is evident within the synchronized regime (medium densities) of traffic flow. The convergence of individual vehicular velocity to the steady-state velocity is realized during either the free-flow regime or the congested regime. During these regimes, values for the velocity-density gradient term are quite smaller. Hence, the instability criterion (2.12) will be violated. But in the absence of

the diffusion and viscosity rates, the threshold for equilibrium traffic corresponds to the value of the sonic speed c . This is given by the expression in equation (2.13) below.

$$\left| \frac{dV_e}{dk} \right| k_e \geq c \quad (2.13)$$

3. MODEL ANALYSIS

The discrete multilane version of the continuous viscous-diffusive model (1.9) is presented here by the introduction of the lane index l , that is

$$\begin{aligned} \frac{\partial k_l(x, t)}{\partial t} + \frac{\partial q_l(x, t)}{\partial x} &= 0 \\ \frac{\partial v_l(x, t)}{\partial t} + v_l(x, t) \frac{\partial v_l(x, t)}{\partial x} &= c \frac{\partial v_l(x, t)}{\partial x} + \frac{V_e(k_l) - v_l(x, t)}{\tau} + D \frac{\partial^2 v_l(x, t)}{\partial x^2} - \phi \frac{\partial v_l(x, t)}{\partial y} \end{aligned} \quad (3.1)$$

$q_l(x, t)$, $k_l(x, t)$ and $v_l(x, t)$ are the flow rate, density, and speed for the l th lane respectively. This equation (3.1) is presented to explain the inter-lane dependency of a multilane flow. Existing models could only explain the association among a limited number of lanes, usually two lanes [12, 24]. Here, an investigation for more than two lanes is presented.

The model is solved numerically because of the computational difficulties associated with the analytical approach to obtaining a solution to this system. Thus, the upwind finite difference scheme is employed to numerically solve this macroscopic system (3.1).

The lane index continuity equation is discretized as

$$k_m^l(n+1) = k_m^l(n) + \Phi v_m^l(n) [k_{m-1}^l(n) - k_m^l(n)] + \Phi k_m^l(n) [v_m^l(n) - v_{m+1}^l(n)] \quad (3.2)$$

The discretized acceleration equation is given by either of the following depending on the intensity of the traffic. When $v_m^l(n) > c$; being a lighter flow regime, then the acceleration equation is given as

$$\begin{aligned} v_m^l(n+1) &= v_m^l(n) + \Phi [c - v_m^l(n)] [v_m^l(n) - v_{m-1}^l(n)] - \Theta \frac{\mu \cdot s_d}{k_m^l(n)} (v_m^l(n) - v_m^{l+1}(n)) \\ &\quad + \frac{\Delta t}{\tau} (V_e - v_m^l(n)) + D \Omega (v_{m-1}^l(n) - 2v_m^l(n) + v_{m+1}^l(n)) \end{aligned} \quad (3.3)$$

In the case of heavy flow ($v_m^l(n) < c$), then the acceleration equation becomes

$$\begin{aligned} v_m^l(n+1) &= v_m^l(n) + \Phi [c - v_m^l(n)] [v_{m+1}^l(n) - v_m^l(n)] - \Theta \frac{\mu_2 \cdot s_d}{k_m^l(n)} (v_m^l(n) - v_m^{l+1}(n)) \\ &\quad + \frac{\Delta t}{\tau} (V_e - v_m^l(n)) + D \Psi (v_{m-1}^l(n) - 2v_m^l(n) + v_{m+1}^l(n)) \end{aligned} \quad (3.4)$$

where $\Delta t / \Delta y = \Theta$, $\Delta t / \Delta x = \Phi$, and $\Delta t / \Delta x^2 = \Psi$. m, n, l are positive integers. $x_m = m \Delta x$, $y_l = l \Delta y$, and $t_n = n \Delta t$. $k_m^l(n) \approx k(x_m, y_l, t_n)$ is the density of vehicles at region m of lane l at time n . $v_m^l(n) \approx v(x_m, y_l, t_n)$ is the velocity of vehicles at position m on lane l at time n . Moreover, the steady-state velocity equation V_e is defined as [10, 11, 15]:

$$V_e = v_f \left\{ 1 - \exp \left[1 - \exp \left(\frac{k_w}{v_f} \left(\frac{k_f}{k_m^l(n)} - 1 \right) \right) \right] \right\} \quad (3.5)$$

k_w is the kinematic wave speed during a heavy traffic domain, v_f and k_f are respectively the maximum speed and density.

For the initial condition, each lane has a specified density value with speed as derived.

$$K^l(x, 0) = \begin{cases} k_1, & \text{if } l = 1 \\ k_2, & \text{if } l = 2 \\ \vdots & \vdots \quad \vdots \\ k_L, & \text{if } l = L \end{cases} \quad V^l(x, 0) = \begin{cases} v(k_1), & \text{if } l = 1 \\ v(k_2), & \text{if } l = 2 \\ \vdots & \vdots \quad \vdots \\ v(k_L), & \text{if } l = L \end{cases}$$

3.1. Simulation Result and Analysis. A graphical solution of this lane-index macro-model is presented in this section. In addition, the information flow of the wave profiles under the perturbation of some key parameters are also presented.

Throughout the simulation, the total distance is taken as $3000m$. A relatively shorter distance is chosen so that one could simultaneously observe both lateral and longitudinal happenings on a given multilane stretch. A simulation for five-lane infrastructure is presented with all vehicles moving along the same direction, with inter-lane interval $\Delta y = 1.5m$. $\Delta x = 300$ and $\Delta t = 4s$ are chosen to satisfy the Courant-Friedrichs-Lewy numerical stability condition (3.6).

$$\max \{v_f - c, q'(k(x, t))\} \cdot \frac{\Delta t}{\Delta x} \leq 1 \tag{3.6}$$

The initial density profile for the five lanes is given as

$$K^l(x, 0) = \begin{cases} 0.50000, & \text{if } l = 1 \\ 0.38750, & \text{if } l = 2 \\ 0.27500, & \text{if } l = 3 \\ 0.16250, & \text{if } l = 4 \\ 0.05000, & \text{if } l = 5 \end{cases}$$

The initial values for the first and last lanes are used as the boundary condition. The lanes are numbered as $l = 1, 2, \dots, 5$. Lane one is the extreme outer lane, while five is the extreme inner lane. The initial density for lane one is denser due to parking on that lane and on the shoulders of the road; this following the no-slip condition of fluid [22, 33]. For the five lane analysis, lanes four and five are the high-speed lanes, while the outer lanes are the low-speed lanes. The following are details of the other parameters [16, 23, 38]:

$$\begin{array}{llll} \mu_2 = 0.0041 & D = 10 & s_d = 0.37 & k_f = 1 \\ c = 11m/s & v_f = 20m/s & \tau = 10s & k_w = 11m/s \end{array}$$

Figure 1 describes some traffic dynamics of a five lane carriageway. It could be observed that the density of the traffic becomes lighter moving from the outer lanes through to the inner lanes. Lane five is less dense, and as such vehicles traversing on this lane have higher velocity compared to the other lanes. Almost all vehicles on lane five could speed up to the maximum, but the situation is different on the outer lanes. This scenario typifies a realistic multilane traffic state in developing countries of which Ghana is not an exception. Here, passenger cars often transverse on the outer lanes, due to their intermittent stopping to pick and drop passengers, making these lanes denser.

Nonetheless, drivers change lanes oftentimes to the left as the density of their driving lane becomes compact. This is depicted through the simulation results with a speed drop and density rise in the higher speed lanes. Deductively, a two-lane highway would easily get clumsy when there is an obstruction on the outer lane. But the situation is different on roadways with arbitrary many lanes. The case of a twenty-lane carriageway is shown in Figure 2. The density of the traffic reduces moving towards the inner lanes because the model hinges on the no-slip condition. For this twenty-lane representation, maximum flow is achieved somewhere around lane fifteen through to twenty.

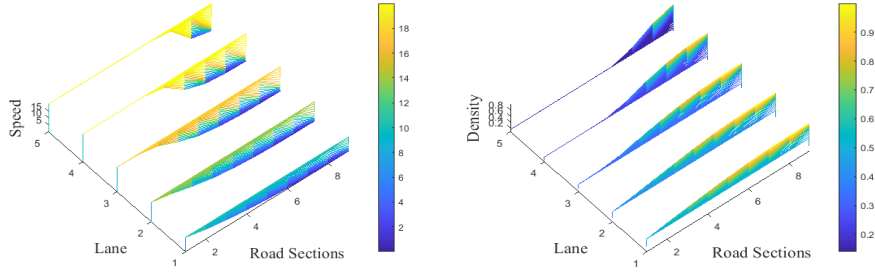


FIGURE 1. Speed and density profiles for a five-lane carriageway

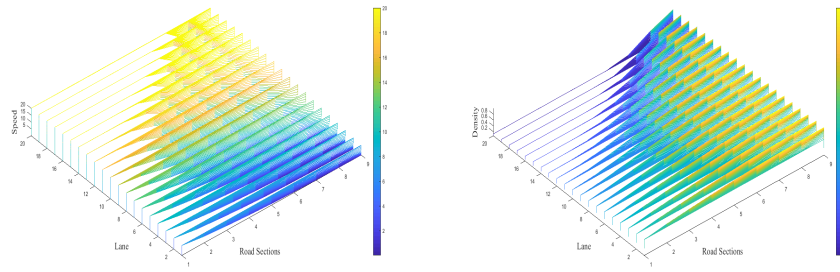
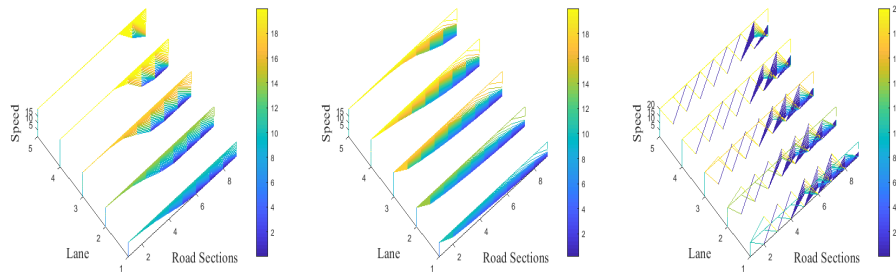


FIGURE 2. Multilane traffic profiles for a twenty-lane carriageway

In Figure 3, the sonic speed c is varied to determine its effect on flow. It was observed that predicting vehicular traffic using this macroscopic model would fail when the value of the sonic speed far exceeds vehicles speed. This is illustrated graphically with $c = 150m/s$. The absence of the anticipation term ($c = 0m/s$) produced quite shorter wave profiles vis-a-vis the benchmark value of $c = 11m/s$ in Figure 1.

FIGURE 3. Multilane speed profiles for $c = 0$, left; $c = 50m/s$, middle; and $c = 150m/s$, right

From the stability criterion (2.12), it was stated that the time taken for traffic to align with the velocity-density dependent value is key in determining the stationarity of the flow. Thus, the adaptation time τ is varied to determine its effect on these multilane wave profiles. From Figure 4, if drivers have enough time to adapt, their speed profiles are finer. That is to say drivers have a longer time to react without any repercussions. Comparing the plot right of Figure 4 to the other on the left, the speed profiles become unstable as τ converges to zero.

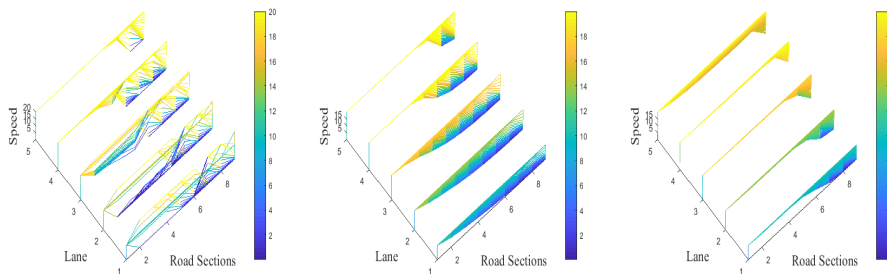


FIGURE 4. Multilane speed profiles for $\tau = 1s$, left; $\tau = 5s$, middle; and $\tau = 120s$, right

A similar perturbation of the lateral viscosity rate is represented in Figure 5. The viscous rate ranges between zero and one; zero denotes the absence of any form of lateral resistance, and one denotes a highly viscous flow. From the simulation plots 5, the effect of viscosity is apparent as μ_2 assumes values closer to the upper limit. It is seen that some amount of lateral obstruction has a consequential effect on the speed of vehicles.

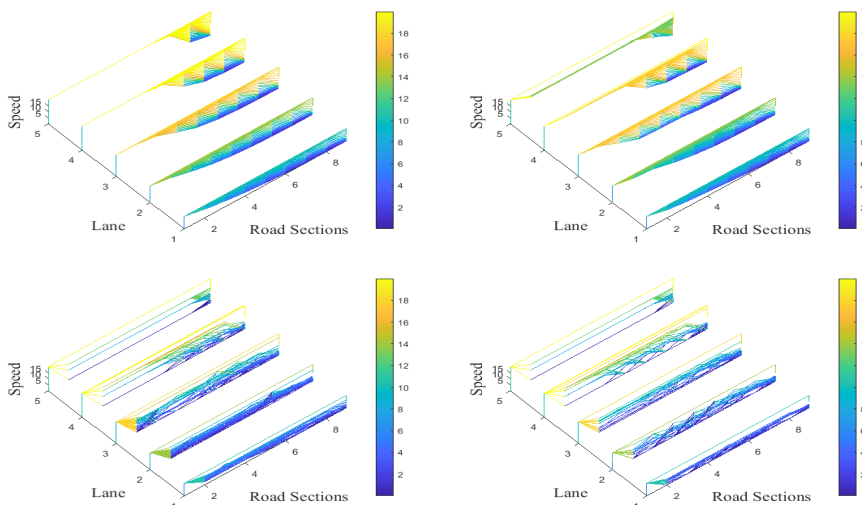


FIGURE 5. Multilane speed profiles under the perturbation of the viscous rate. Top left: $\mu_2 = 0$, top right: $\mu_2 = 0.041$, bottom left: $\mu_2 = 0.41$, and bottom right: $\mu_2 = 1.00$

From Figure 6, the prediction of traffic using this multilane model was found to be feasible whether diffusion was present or not. The diffusive term was barely substantiated in this simulation work. Nonetheless, a highly enormous value showed inclinations of abnormal flow.

4. CONCLUSION

Macroscopic traffic models of second-order consist of the continuity equation and the dynamic velocity equation. The dynamic velocity equation was introduced to rectify the shortcomings of the continuity equation. The components of the dynamic velocity equation are convection, anticipation, relaxation, diffusion, and viscosity. In this paper, a new macro-model that features all these dynamic speed quantities is presented. Then after, the linear-stability condition of the new continuum second-order

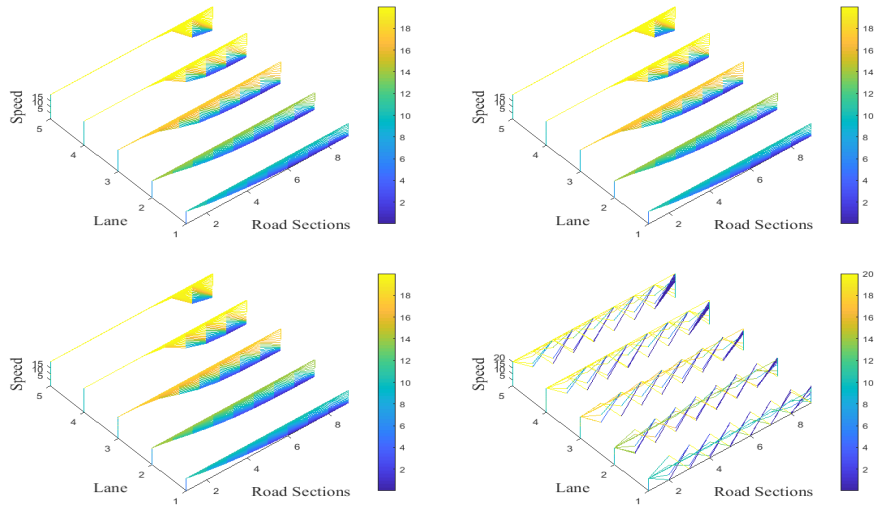


FIGURE 6. Multilane speed profiles under the perturbation of the diffusion rate. Top left: $D = 0$, top right: $D = 50$, bottom left: $D = 500$, and bottom right: $D = 15000$

model was determined through the analysis of wave profiles. The gradient of the velocity-density curve, the average density, and the sonic speed were found to be the determining variables for either stable or unstable flow. The proposed anisotropic model was again recast as a lane-indexed model and was solved numerically using the upwind finite difference scheme. This reformulation was done to remove the restriction on the proposed model as being single-piped. The viscosity rate, anticipation, diffusion, and relaxation time were perturbed to examine its effect on flow. By the simulation plots, it was observed that a smaller relaxation time, a larger anticipation rate, and a unit size lateral viscosity rate have an adverse effect on the flow rate. The speed profiles were observed to be awkward for some range of values. However, the diffusive term did not have any substantial impact on the speed profiles, except for the case of extremely large values.

REFERENCES

- [1] W. Ai, N. Li, and R. Tian, *Stability analysis of a viscous continuous traffic flow model*, ITM Web of Conferences, EDP Sciences, **45**, 2022.
- [2] W. Ai, Y. Su, T. Xing, and D. Liu, *Bifurcation analysis of modified density gradient continuum traffic model*, Mod. Phys. Lett. B **35** (2021), 2150475.
- [3] A. Aw and M. Rascle, *Resurrection of “second order” models of traffic flow*, SIAM J. Appl. Math. **60** (2000), 916–938.
- [4] M. Bouadi, B. Jia, R. Jiang, X. Li, and Z. Gao, *Traffic flow stability in stochastic second-order macroscopic continuum model*, arXiv preprint arXiv:2204.13937 (2022).
- [5] B. Cen, Y. Xue, Y. Qiao, Y. Wang, W. Pan, and H. He, *Global stability and bifurcation of macroscopic traffic flow models for upslope and downslope*, Research square preprint (2022).
- [6] F. A. Chiarello, *An overview of non-local traffic flow models, mathematical descriptions of traffic flow: micro, macro and kinetic models*, Springer (2021), 79–91.
- [7] G. M. Coclite, N. D. Nitti, M. Garavello, and F. Marcellini, *Vanishing viscosity for a 2×2 system modeling congested vehicular traffic*, Netw. Heterog. Media **16** (2021), 413–426.

- [8] G. M. Coclite, N. D. Nitti, A. Keimer, and L. Pflug, *Singular limits with vanishing viscosity for nonlocal conservation laws*, *Nonlinear Anal.* **211** (2021), 112370.
- [9] C. F. Daganzo, *Requiem for second-order approximations of traffic flow*, *Transp. Res. B: Methodol* **29** (1995), 277–286.
- [10] J. M. Del Castillo and F. G. Benitez, *On functional form of the speed-density relationship - I: General theory*, *Transp. Res. B: Methodol.* **29** (1995), 373–389.
- [11] J. M. Del Castillo and F. G. Benitez, *On functional form of the speed-density relationship - II: Empirical investigation*, *Transp. Res. B: Methodol.* **29** (1995), 391–406.
- [12] A. I. Delis, I. K. Nikolos, and M. Papageorgiou, *Macroscopic modelling and simulation of multi-lane traffic*, *IEEE 18th International Conference on Intelligent Transportation Systems*, (2015), 2213–2218.
- [13] A. Ferrara, S. Sacone, and S. Siri, *Freeway traffic modelling and control*, Springer, 2018.
- [14] G. O. Fosu, F. T. Oduro, and C. Caligaris, *Multilane analysis of a viscous second-order macroscopic traffic flow model*, *SN PDE* **2** (2021).
- [15] G. O. Fosu, E. Akweittay, J. M. Opong, and M. E. Otoo, *Vehicular traffic models for speed-density-flow relationship*, *J. Math. Model.* **8** (2020), 241–255.
- [16] G. O. Fosu and F. T. Oduro, *Two dimensional anisotropic macroscopic second-order traffic flow model*, *J. Appl. Comput. Mech.* **19** (2020), 59–71.
- [17] G. O. Fosu, J. M. Opong, B. E. Owusu, and S. M. Naandam, *Modeling road surface potholes within the macroscopic flow framework*, *Math. Appl. Sci. Eng.* **3** (2022), 106–118.
- [18] H. Ge and S. Lo, *The kdv-burgers equation in speed gradient viscous continuum model*, *Phys. A: Stat. Mech. Appl.* **391** (2012), 1652–1656.
- [19] D. Helbing and A. F. Johansson, *On the controversy around Daganzo’s requiem for and Aw-Rasclé’s resurrection of second-order traffic flow models*, *Eur. Phys. J. B* **69** (2009), 549–562.
- [20] M. Herty, A. Fazekas, and G. Visconti, *A two-dimensional data-driven model for traffic flow on highways*, *AIMS* **13** (2018), 217–240.
- [21] M. Herty, S. Moutari, and G. Visconti, *Macroscopic modeling of multi-lane motorways using a two-dimensional second-order model of traffic flow*, *SIAM* **78** (2018), 2252–2278.
- [22] W. S. Janna, *Introduction to fluid mechanics*, CRC Press. Taylor & Francis Group, 2010.
- [23] R. Jiang, Q. S. Wu, and Z. J. Zhu, *A new continuum model for traffic flow and numerical tests*, *Transp. Res. B: Methodol.* **36** (2002), 405–419.
- [24] M. H. Kabir and L. S. Andallah, *Numerical solution of a multilane traffic flow model*, *GANIT J. Bangladesh Math. Soc.* **33** (2013), 25–32.
- [25] B. S. Kerner and P. Konhäuser, *Structure and parameters of clusters in traffic flow*, *Phys. Rev. E* **50** (1994), 54–83.
- [26] Z. H. Khan, W. Imran, T. A. Gulliver, K. S. Khattak, Z. Wadud, and A. N. Khan, *An anisotropic traffic model based on driver interaction*, *IEEE Access* **8** (2020), 66799–66812.
- [27] Z. H. Khan, T. A. Gulliver, W. Imran, K. S. Khattak, A. B. Altamimi, and A. Qazi, *A macroscopic traffic model based on relaxation time*, *Alex. Eng. J.* **61** (2022), 585–596.
- [28] Z. H. Khan, T. A. Gulliver, H. Nasir, A. Rehman, and K. Shahzada, *A macroscopic traffic model based on driver physiological response*, *J. Eng. Math.* **115** (2019), 21–41.
- [29] R. Kühne, *Macroscopic freeway model for dense traffic-stop-start waves and incident detection. in J. Vollmuler and R. Hamerslag, editors, Proceedings of the 9th International Symposium on Transportation and Traffic Theory (ISTTT9)*, 1984, 21–42.
- [30] C. Lustrì, *Continuum modelling of traffic flow*, (2010).

- [31] H. J. Payne, *Models of freeway traffic and control*, In: G. A. Bekey (ed.) *Mathematical Models of Public Systems* (Simulation Council, La Jolla, CA) **1** (1971), 51–61.
- [32] M. Rasclé, *An improved macroscopic model of traffic flow: derivation and links with the Lighthill Whitham model*, *Math. Comput. Model.* **35** (2002), 581–590.
- [33] M. Rieutord, *Fluid dynamics an introduction*, Springer Cham Heidelberg New York Dordrecht London, 2015.
- [34] M. H. Sadeghian, M. Gachpazan, N. Davoodi, and F. Toutounian, *A macroscopic second order model for air traffic flow*, *J. Math. Model.* **8** (2020), 41–54.
- [35] S. Schochet, *The instant-response limit in whitham’s nonlinear traffic-flow model: uniform well-posedness and global existence*, *Asymptot. Anal.* **1** (1988), 263–282.
- [36] M. Treiber and A. Kesting, *Traffic flow dynamics; data, models and simulation*, Springer-Verlag Berlin Heidelberg, 2013.
- [37] G. B. Whitham, *Linear and nonlinear waves*, John Wiley and Sons, New York, 1974.
- [38] L. Yu, T. Li, and Z. Shi, *The effect of diffusion in a new viscous continuum traffic model*, *Phys. Lett. A* **374** (2010), 2346–2355.
- [39] H. M. Zhang, *A non-equilibrium traffic model devoid of gas-like behavior*, *Transp. Res. B: Methodol.* **36** (2002), 275–290.
- [40] P. Zhang, Y. Xue, Y. Zhang, X. Wang, and B. Cen, *A macroscopic traffic flow model considering the velocity difference between adjacent vehicles on uphill and downhill slopes*, *Mod. Phys. Lett. B* (2020), 2050217.
- [41] Y. Zhang, W. Ai, and D. Liu, *Analysis of equilibrium point based on nonlinear traffic flow model*, *ITM Web of Conferences, EDP Sciences*, **45**, 2022, 01055.
- [42] S. Zheng, R. Jiang, B. Jia, J. Tian, and Z. Gao, *Impact of stochasticity on traffic flow dynamics in macroscopic continuum models*, *Transp. Res. Rec.* **2674** (2020), 690–704.

CORRESPONDING AUTHOR, DEPARTMENT OF MATHEMATICS, KWAME NKRUMAH UNIVERSITY OF SCIENCE AND TECHNOLOGY, KUMASI, GHANA

Email address: gabriel.of@knust.edu.gh

DEPARTMENT OF APPLIED MATHEMATICS, KOFORIDUA TECHNICAL UNIVERSITY, GHANA

Email address: albert.adu-sackey@ktu.edu.gh

DEPARTMENT OF MATHEMATICS, KWAME NKRUMAH UNIVERSITY OF SCIENCE AND TECHNOLOGY, KUMASI, GHANA

Email address: jaackora-prah.cos@knust.edu.gh